Journal of Solid State Chemistry 182 (2009) 2743–2747

Contents lists available at ScienceDirect

Journal of Solid State Chemistry

journal homepage: www.elsevier.com/locate/jssc

The hydrothermal decomposition of calcium monosulfoaluminate 14-hydrate to katoite hydrogarnet and β-anhydrite: An in-situ synchrotron X-ray diffraction study

Nicola Meller, Konstantinos Kyritsis, Christopher Hall *

School of Engineering and Centre for Science at Extreme Conditions, The University of Edinburgh, The King's Buildings, Edinburgh EH9 3JZ, UK

ARTICLE INFO

Article history:
Received 7 April 2009
Received in revised form
10 July 2009
Accepted 18 July 2009
Available online 25 July 2009

Keywords:
Calcium monosulfoaluminate hydrate
Hydrothermal decomposition
Synchrotron diffraction
Layer compounds

ABSTRACT

We apply in-situ synchrotron X-ray diffraction to study the transformation of calcium monosulfoaluminate 14-hydrate $Ca_4Al_2O_6(SO_4)\cdot 14H_2O$ [monosulfate-14] to hydrogarnet $Ca_3Al_2(OH)_{12}$ on the saturated water vapor pressure curve up to 250 °C. We use an aqueous slurry of synthetic ettringite $Ca_6Al_2(SO_4)_3(OH)_{12}\cdot 26H_2O$ as the starting material; on heating, this decomposes at about 115 °C to form monosulfate-14 and bassanite $CaSO_4\cdot 0.5H_2O$. Above 170 °C monosulfate-14 diffraction peaks slowly diminish in intensity, perhaps as a result of loss of crystallinity and the formation of an X-ray amorphous meta-monosulfate. Hydrogarnet nucleates only at temperatures above 210 °C. Bassanite transforms to β-anhydrite (insoluble anhydrite) at about 230 °C and this transformation is accompanied by a second burst of hydrogarnet growth. The transformation pathway is more complex than previously thought. The mapping of the transformation pathway shows the value of rapid in-situ time-resolved synchrotron diffraction.

1. Introduction

The calcium aluminate monosulfate hydrates $Ca_4Al_2O_6(SO_4)\cdot nH_2O$ (where $n = 8$–14) are ternary layered double hydroxides [1] with structures related to brucite, hydrotalcite and hydrocalumite. These materials are of particular interest because of their rich intercalation chemistry and structural diversity [2,3]. The best characterized is the 12-hydrate which occurs naturally as the mineral kuzelite [4], the crystal structure of which has been determined by Allmann [5]. The monosulfate hydrates form in portland cements under normal and hydrothermal conditions [6], as does the closely related chloride analog, Friedel's salt [7]. These monosulfate hydrates (simply called monosulfates in the cement chemistry literature) are often designated as AFm phases (the acronym indicating that lattice substitution of Al by Fe may occur).

The monosulfates form in cement in two ways. The first is by reaction of the cement clinker aluminate and aluminoferrite phases ($Ca_3Al_2O_6$, $Ca_4(Al,Fe)_2O_7$) with ettringite ($Ca_6Al_2(SO_4)_3(OH)_{12}\cdot 26H_2O$) in sulfate-deficient environments. The second is by thermal decomposition of ettringite, when ettringite decomposes to monosulfate $Ca_4Al_2O_6(SO_4)\cdot nH_2O$ and (it is generally assumed) bassanite $CaSO_4\cdot 0.5H_2O$ by the reaction:

$$Ca_6Al_2(SO_4)_3(OH)_{12}\cdot 26H_2O \rightarrow Ca_4Al_2O_6(SO_4)\cdot nH_2O + 2CaSO_4\cdot mH_2O + (32-n-2m)H_2O \quad (1)$$

where $n = 10$–14 depending on water activity, $m = 0.5$ or 0. n is observed to be 14 when a saturated vapor pressure of water is maintained [8–10]. The calcium sulfate product phase may be either the hemihydrate bassanite ($m = 0.5$) or γ-anhydrite ($m = 0$), the so-called 'soluble anhydrite'. It is generally assumed to be bassanite [8].

The thermal decomposition of ettringite has been the subject of discussion for many years and the temperature of thermal decomposition depends on both pressure and humidity [8,11]. In the absence of water or at low water activity, ettringite decomposes first to meta-ettringite [12–15], an X-ray amorphous material with some long range order. If saturated vapor pressure is maintained, the temperature of decomposition of ettringite according to Eq. (1) is generally considered to lie in the range 110–120 °C, the temperature of decomposition apparently increasing with pressure [8,11,16,17].

There is a wealth of literature available on the thermal decomposition of ettringite, but in contrast relatively little is known about the thermal decomposition of the monosulfate phase. Monosulfate-14 decomposes to a katoitic hydrogarnet

* Corresponding author.
E-mail address: christopher.hall@ed.ac.uk (C. Hall).

0022-4596/$ - see front matter © 2009 Elsevier Inc. All rights reserved.
doi:10.1016/j.jssc.2009.07.029

$Ca_3Al_2(OH)_{12}$ and so-called 'insoluble anhydrite' β-$CaSO_4$ by the following formal reaction:

$$Ca_4Al_2O_6(SO_4)\cdot 14H_2O \rightarrow Ca_3Al_2(OH)_{12}+CaSO_4\cdot mH_2O+(8-m)H_2O \quad (1)$$

where $m = 0.5$ or 0. It has been reported that this reaction occurs above 190 °C under saturated water vapor pressure conditions [11] and that hydrogarnet is observed as the major phase at 232 °C [18]. However the exact temperature at which decomposition occurs remains elusive. The aim of the work we describe is to track the thermal decomposition of monosulfate using a novel in-situ X-ray diffraction technique. This approach not only yields the temperature of decomposition but also gives us information on the kinetics of the decomposition reaction.

2. Experimental section

2.1. Monosulfate synthesis

A slurry of ettringite can be produced from a stoichiometric mixture of reagent grade calcium hydroxide and aluminum sulfate hydrate by a method [8] similar to that originally described by Atkins et al. [19]. Normally in this synthesis the slurry is left to age for some hours before washing and filtering; however we use the slurry immediately after mixing and before any crystal ripening. This provides smaller crystals of ettringite, which can be loaded more easily into capillaries. X-ray diffraction of the crystalline product shows that we make a phase-pure ettringite suspension [Meller and Kyritsis unpublished data]. In order to produce monosulfate the sample is simply heated to decompose ettringite to monosulfate and bassanite [8]. This yields the 14-hydrate monosulfate $Ca_4Al_2O_6(SO_4)\cdot 14H_2O$, as observed in previous experiments [8] where saturated water vapor pressure is maintained. To synthesize the monosulfate off-line risks loss of hydration water during drying or handling to form the 12-hydrate $Ca_4Al_2O_6(SO_4)\cdot 12H_2O$, the product generally reported in ex-situ experiments [11,17]. From Eq. (1) we see that our in-situ slurry method introduces bassanite into the system during the dehydration of ettringite but this is the price we pay to be sure that we start with a fully hydrated monosulfate-14. In any event, bassanite or other simple calcium sulfate mineral is also generally present in the hydrothermal portland cement systems to which our study relates.

2.2. Experimental methods

All monosulfate decomposition experiments were run on Station MPW6.2 at the UK Synchrotron Radiation Source SRS at Daresbury Laboratories [20–22]. This is a monochromated angle-dispersive diffractometer beamline with a tunable X-ray wavelength which we set at 0.1 nm. This wavelength was chosen to achieve greater penetration through the sample and hence higher quality data. The disadvantage of using higher energies is that photon intensity decreases so a balance between energy and intensity must be struck. The diffracted X-rays were collected by a RAPID2 wide-angle detector, calibrated using silicon powder in a 0.7 mm external dia soda lime capillary of wall thickness 0.01 mm. The highest d-spacing visible to the detector was 7.7 Å (d^{-1} 1.3 nm^{-1}) but data at $d > 6.7$ Å ($d^{-1} < 1.5$ nm^{-1}) were too noisy to be of use. Hence all diffraction datasets have a maximum d-spacing of 6.7 Å ($d^{-1} < 1.5$ nm^{-1}). While this range excludes the intense high d-spacing ettringite 0 0 1 and monosulfate 0 0 3 peaks, all the other major peaks were observable.

The sample was mounted on a purpose-built stage based on a design by Norby [23] and heated by means of a hot air stream. This stage has been used successfully at temperatures up to 170 °C for cementitious systems [24,25] but here we push the limits of the stage, using thicker capillaries, to 250 °C. The capillaries are made from quartz glass and have a 1 mm external dia and a wall thickness of 0.02 mm. The ettringite slurry is loaded into the capillary using a 0.5 mm dia soda lime capillary, with a wall thickness of 0.01 mm, fixed to a syringe. The temperature of the sample is measured with a K-type thermocouple positioned close to the tip of the capillary. The original stage design [23] was modified to avoid temperature variations across the nozzle by the addition of a copper sleeve (Fig. 1). The capillary containing the ettringite slurry is first aligned in the beam and the copper tube is then moved into place over the capillary. The sample was oscillated over a 120° arc to reduce settling and improve particle statistics.

Once in position 40 bar nitrogen gas pressure was applied to the capillary to suppress boiling and loss of water; however it should be noted that the sample can only be kept wet if a cold slug of fluid is positioned between the hot reacting zone and the nitrogen gas. If no such cold slug exists water vapor escapes from the sample–nitrogen interface and the sample dries out, and we see the ettringite structure collapse to X-ray amorphous meta-ettringite instead of decomposing to monosulfate [12–15].

Samples were ramped from ambient temperature to 250 °C over 2 h and a pattern was collected every 30 s. Six samples were run to verify the method; we included two samples with silica additions, in the form of either quartz or silicic acid. Silica was

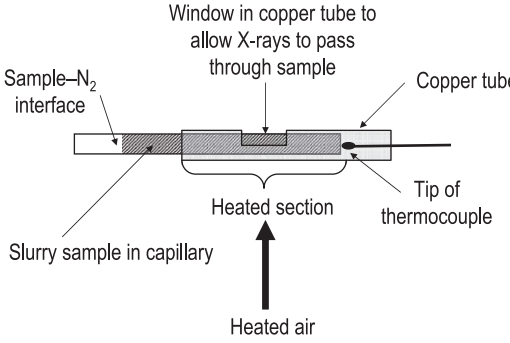

Fig. 1. Sketch of sample in capillary to show modified stage of Norby [22] with a copper tube. The copper tube removes temperature variations across the sample and ensures that the thermocouple and the section of capillary observed by the X-ray beam are at the same temperature. Note the air/slurry interface lies outside the heated zone to prevent boiling off and loss of water during heating.

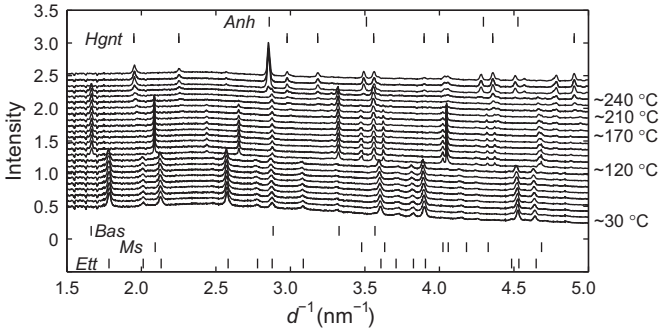

Fig. 2. X-ray diffraction patterns collected in-situ showing the thermal decomposition of ettringite (*Ett*) to first form monosulfate-14 (*Ms*) and bassanite (*Bas*), and then to form hydrogarnet (*Hgnt*) and β-anhydrite (*Anh*). Patterns were collected every 30 s for 2 h and temperature was ramped from ambient to 250 °C over 2 h. Every 20th pattern is plotted for clarity and the time interval between each pattern is approx. 10 min.

Table 1
ICDD reflections used to identify phases.

Phase	Alternative name	Formula	Crystal system	ICDD pattern used for identification	Peaks fitted	d (Å)	d^{-1} (nm^{-1})
Ettringite	AFt	$Ca_6Al_2(SO_4)_3(OH)_{12}\cdot 26H_2O$	Hexagonal	41–1451	1 1 0	5.61	1.78
					1 1 4	3.87	2.58
					2 1 6	2.56	3.91
					2 2 6	2.21	4.53
Monosulfate-14	AFm	$Ca_4Al_2O_6(SO_4)\cdot 14H_2O$	Hexagonal	42–62	0 0 6	4.78	2.09
					1 1 0	2.88	3.48
					1 0 1 0	2.48	4.02
Hydrogarnet	Katoite	$Ca_3Al_2(OH)_{12}$	Cubic	24–217	2 1 1	5.13	1.95
					6 1 1	2.04	4.90
Bassanite	Hemihydrate	$CaSO_4\cdot 0.5H_2O$	Monoclinic	41–244	2 0 0	6.01	1.66
					4 0 0	3.01	3.33
Insoluble anhydrite	β-Anhydrite	$CaSO_4$	Orthorhombic	37–1496	0 1 2	2.85	3.51

added to the ettringite to observe possible effects of silica on the formation of the aluminate phases during cement hydration at elevated temperature. As no differences were observed between samples with and without silica, the samples with silica additions are treated simply as repeat experiments.

The width of the diffraction peaks of well crystallized components is typically $<0.01\,\mathrm{nm}^{-1}$ (full-width half-maximum) in $1/d$ reciprocal space. The peaks are adequately represented by Gaussian lineshapes. No corrections were made for the slow decay of the synchrotron beam current since experiments were of short (2 h) duration. Many peaks overlap (Fig. 2) and so the choice of suitable peaks was restricted. Where possible more than one peak was fitted for each phase (Table 1) but in the case of anhydrite this was not possible because of severe peak overlap, indistinct background or an insufficient number of data points across the peak.

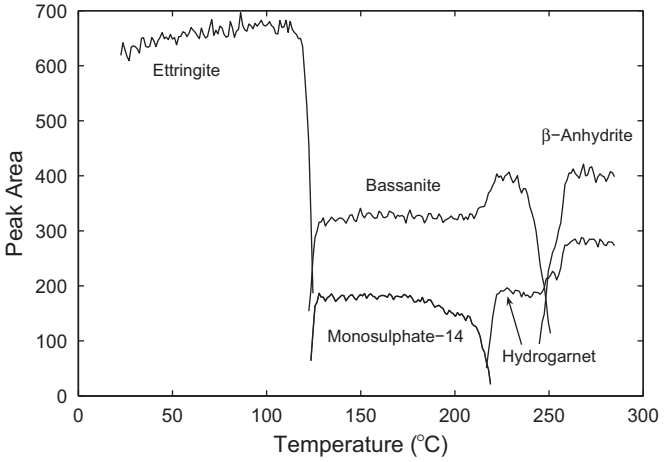

Fig. 3. Peak area versus temperature for ettringite 1 1 0; monosulfate 1 0 1 0; bassanite 2 0 0; hydrogarnet 6 1 1; and insoluble anhydrite 0 1 2 peaks.

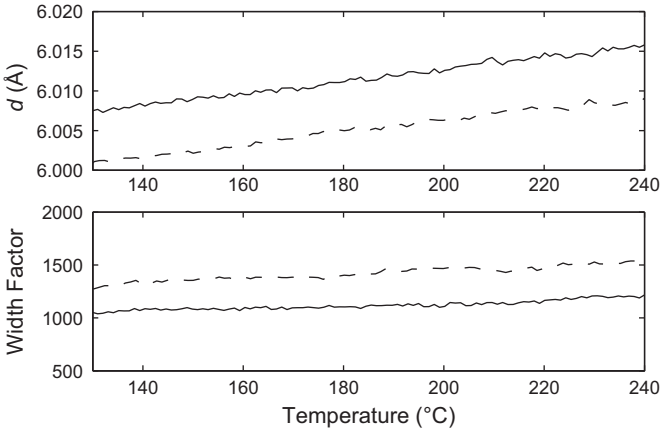

Fig. 4. Peak position (a) and peak width (b) versus temperature for the bassanite peak at 6.01 Å ($1/d$ 1.66 nm^{-1}). Two experiments are shown: one without silica additions (solid) and one with silica additions (dashed). There is no obvious discontinuity in either peak position or peak width in the temperature range 130–240 °C.

3. Results and discussion

3.1. General features

The diffraction patterns (Fig. 2) in all experiments show clearly that ettringite decomposes to monosulfate-14 and a simple calcium sulfate, which *a priori* may be bassanite or soluble γ-anhydrite or a mixture of both (Eq. (1)); and that monosulfate-14 decomposes ultimately to hydrogarnet and insoluble β-anhydrite at higher temperatures (Eq. (2)). If the peak areas are plotted against temperature (Fig. 3) we see that while the decomposition of ettringite to monosulfate and bassanite/γ-anhydrite is a rather brief event spanning about 7 min (or a 10 °C temperature range) the decomposition of monosulfate is more complex and extended. While there are some minor variations in the six experimental runs, the broad picture is the same in each experiment. The decomposition of ettringite starts at about 115 °C, as previously reported [8] for the saturated water vapor system.

3.2. The difficulty of distinguishing between bassanite and soluble anhydrite

The crystal structure and diffraction patterns of bassanite and soluble γ-anhydrite are closely similar. Bassanite has a monoclinic structure composed of columns of Ca–O polyhedra and sulfate tetrahedral [26], with water molecules sited in the channels. The γ-anhydrite structure is similar except that the water molecules are absent and the zeolitic channels are empty. The structure has higher symmetry and is hexagonal. However because their diffraction patterns are so similar, bassanite and γ-anhydrite can be distinguished in powder X-ray patterns only by small peak shifts [20] or by the presence or absence of a few weak reflections [8]. The latter approach is difficult to employ here because of poor signal to noise ratio. Hall et al. [8] in an earlier in-situ study of

ettringite decomposition concluded from analysis of a number of peak intensities, positions and absences that the mineral formed was bassanite. In the present study, we have made a careful analysis of the *d*-spacing of the diagnostic line at 6.01 Å as temperature increases. Fig. 4a shows no obvious discontinuity such as observed by Gonzalez-Sáborido [21]. The *d*-spacing increases slightly with temperature and the change ($12 \times 10^{-6}\,K^{-1}$) is of the magnitude expected for a pure lattice thermal expansion. We conclude that we see no evidence of a structural transformation in this phase from its first appearance at around 120 °C until it finally transforms to β-anhydrite at about 240 °C. Transformation of bassanite to γ-anhydrite with increasing temperature has been reported using X-ray [20] and infra-red methods [27], but in both cases the material was dry and a progressive dehydration of bassanite is therefore not surprising. In the case we report here the sample is sealed and contains free water throughout. In a recent synchrotron diffraction study [21] of the dehydration of pure gypsum with excess water in a sealed capillary, the bassanite→γ-anhydrite transformation was observed to occur only at and above 240 °C. We consider that the available data suggest that in our system bassanite rather than γ-anhydrite is the intermediate calcium sulfate phase present.

3.3. Decomposition of monosulfate-14

Monosulfate and bassanite peak areas remain constant for about 32 min (from about 120–170 °C). At about 170 °C, the monosulfate peak areas begin to decrease and this loss of intensity becomes increasingly pronounced as the temperature rises to about 200 °C. No new phases appear and there is no increase in the amount of co-existing crystalline bassanite. If monosulfate were dissolving, the calcium and sulfate ion content of the solution would also increase, and in that case it is hard to understand how the bassanite peak areas could remain constant. An alternative and better explanation is that the decrease in monosulfate peak intensities is caused by a progressive decrease in crystallinity as a result of partial loss of interlayer water and resulting structural disorder. In forming such a *meta-monosulfate* some additional free water is released which maintains the hydration state of the bassanite.

At about 210 °C hydrogarnet nucleates and grows rapidly, presumably by conversion of the meta-monosulfate. The hydrogarnet peak area reaches a plateau at about 220 °C (Figs. 2 and 3). The rapid growth of hydrogarnet is accompanied by an increase of about 25% in the amount of bassanite as calcium, sulfate and water are released from the monosulfate. This increase in bassanite is only about half the amount $CaSO_4$ required by the stoichiometry of Eq. (2), suggesting that the conversion of monosulfate is incomplete at the hydrogarnet plateau. Eq. (2) also shows that free water is also released by the monosulfate conversion, so there is no reason to suppose that the bassanite is dehydrated to γ-anhydrite. The absence of a shift in the diagnostic reflection supports this.

As temperature continues to rise we see the first appearance of β-anhydrite at about 230 °C. This conversion is known to occur via a through-solution mechanism [27]. It appears to be accompanied by an additional burst of hydrogarnet growth at about 240 °C. The reason for additional hydrogarnet growth is unclear. The change in peak area is probably too sharp to indicate settling. As we have noted, it is possible that some amorphous meta-monosulfate not detectable by X-ray diffraction is present, and if so the decomposition of this supplies the Al to form the additional hydrogarnet. It is also unclear why a burst of hydrogarnet growth occurs at the same time as the conversion of bassanite to insoluble β-anhydrite. The solubility of bassanite falls with increasing temperature and is similar to that of β-anhydrite at about 200 °C [28], so little change is expected in solution composition as this conversion proceeds.

4. Conclusions

In-situ synchrotron X-ray diffraction has shown that ettringite in a sealed environment with free water first decomposes to monosulfate and bassanite at around 115 °C; and ultimately transforms to hydrogarnet and insoluble β-anhydrite above about 230 °C. In the temperature range 170–250 °C we observe a sequence of intermediate changes:

1. Monosulfate-14 becomes less crystalline over the temperature range 170–220 °C, probably as the result of some loss of interlayer water.
2. There is no evidence of the formation of γ-anhydrite at the expense of bassanite.
3. Hydrogarnet nucleates and grows at temperatures >210 °C.
4. As the hydrogarnet appears, there is a corresponding increase in the amount of bassanite.
5. Bassanite converts to insoluble β-anhydrite from 230 to 250 °C and this coincides with a further episode of hydrogarnet growth.

Previous attempts at elucidating this sequence of reactions have only touched on part of the story. While stoichiometric equations describe the overall transformation, in-situ observations reveal much detail and show that the steps from reactant to product are far from simple.

Acknowledgments

We are grateful to the UK Engineering and Physical Sciences Research Council for financial support and synchrotron beamtime; to C.M. Martin, G. Clarke, D. Coleman (Daresbury Laboratory) for their help with synchrotron facilities; to G. Giriat (University of Edinburgh) for assistance with experiments; to R. Hogg and D. Archibald (University of Edinburgh) for technical help building the sample stage. We thank Simon Jacques, Alejandro González Saborido and Paul Barnes (University College London) for providing unpublished data on the thermal decomposition of gypsum.

References

[1] H. Pöllmann, N. Jb, Miner. Abh. 182 (2) (2006) 173–181.
[2] D.G. Evans, R.C.T. Slade, in: D.M.P. Mingos, X. Duan, D.G. Evans (Eds.), Structural Aspects of Layered Double Hydroxides, Springer, Berlin, 2006, pp. 1–87.
[3] A.I. Khan, D. O'Hare, J. Mater. Chem. 12 (11) (2002) 3191–3198.
[4] H. Pöllmann, T. Witzke, H. Kohler, N. Jb, Miner. Monat. 9 (1997) 423–432.
[5] R. Allmann, N. Jb, Miner. Monat. (1977) 136–143.
[6] T. Matschei, B. Lothenbach, F.P. Glasser, Cem. Concr. Res. 37 (2) (2007) 118–130.
[7] U.A. Birnin-Yauri, F.P. Glasser, Cem. Concr. Res. 28 (12) (1998) 1713–1723.
[8] C. Hall, P. Barnes, A.D. Billimore, A.C. Jupe, X. Turrillas, J. Chem. Soc. Faraday Trans. 92 (1996) 2125–2129.
[9] N. Meller, C. Hall, A.C. Jupe, S.L. Colston, S. Jacques, P. Barnes, J. Phipps, J. Mater. Chem. 14 (3) (2004) 428–435.
[10] S.L. Colston, P. Barnes, A. Jupe, S. Jacques, C. Hall, P. Livesey, J. Dransfield, N. Meller, Cem. Concr. Res. 35 (12) (2005) 2223–2232.
[11] V. Satava, O. Veprek, J. Am. Ceram. Soc. 58 (1975) 357–359.
[12] Q. Zhou, F.P. Glasser, Cem. Concr. Res. 31 (2001) 133–1339.
[13] Q. Zhou, E.E. Lachowski, F. Glasser, Cem. Concr. Res. 34 (2004) 703–710.
[14] M.R. Hartman, S.K. Brady, R. Berliner, M.S. Conradi, J. Solid State Chem. 179 (2006) 1259–1272.
[15] Y. Shimada, J.F. Young, Adv. Cem. Res. 13 (2) (2001) 77–81.
[16] K. Ogawa, D.M. Roy, Cem. Concr. Res. 11 (1981) 741–750.
[17] I. Nerád, S. Šaušova, L. Ševula, Cem. Concr. Res. 24 (1994) 259–266.

[18] P.K. Mehta, J. Am. Ceram. Soc. 55 (1972) 55–56.
[19] M. Atkins, F.P. Glasser, A. Kindness, Cem. Concr. Res. 22 (1992) 241–246.
[20] R.J. Cernik, P. Barnes, G. Bushnell-Wye, A.J. Dent, G.P. Diakun, J.V. Flaherty, G.N. Greaves, E.L. Heeley, W. Helsby, S.D.M. Jacques, T. Rayment, A. Ryan, C.C. Tang, N.J. Terrill, J. Synchrotron Radiat. 11 (2004) 163–170.
[21] A. González Saborido, Ph.D. Thesis, University of London, 2009.
[22] C.C. Tang, C.M. Martin, D. Laundy, S.P. Thompson, G.P. Diakun, R.J. Cernik, Nucl. Instrum. Meth. B 222 (3–4) (2004) 659–666.
[23] P. Norby, J. Am. Chem. Soc. 119 (1997) 5215–5221.
[24] A.N. Christensen, N.V.Y. Scarlett, I.C. Madsen, T.R. Jensen, J. Hanson, Dalton Trans. (2003) 1529–1536.
[25] A.N. Christensen, T.R. Jensen, J.C. Hanson, J. Solid State Chem. 177 (2004) 1944–1951.
[26] G.A. Lager, T. Armbruster, F.J. Rotella, J.D. Jorgensen, D.G. Hinks, Am. Mineral. 69 (1984) 910–918.
[27] A. Putnis, B. Winkler, L. Fernandez-Diaz, Mineral. Mag. 54 (1990) 123–128.
[28] G. Azimi, V.G. Papangelakis, J.E. Dutrizac, Fluid Phase Equilib. 260 (2007) 300–315.